PRAMANA — journal of physics

Vol. 79, No. 2
August 2012
pp. 327–335

Electronic structure and equilibrium properties of hcp titanium and zirconium

B P PANDA
Department of Physics, Begunia College, Begunia 752 062, India
E-mail: nulu22@yahoo.com

MS received 21 May 2011; revised 17 November 2011; accepted 1 March 2012

Abstract. The electronic structures of hexagonal-close-packed divalent titanium (3-d) and zirconium (4-d) transition metals are studied by using a non-local model potential method. From the present calculation of energy bands, Fermi energy, density of states and the electronic heat capacity of these two metals are determined and compared with the existing results in the literature.

Keywords. Electronic structure; titanium and zirconium; model potential calculation.

PACS Nos 71.20.–b; 71.15.Dx

1. Introduction

The transition metals, titanium ($Z = 22$) and zirconium ($Z = 40$), which are in the same column of periodic table, crystallize in the hexagonal-close-packed (hcp) structure. The hcp structure is very common among the metals and the two atoms per unit cell gives an electronic structure which is more complex than that of the cubic metals. Quite a few theoretical calculations of the electronic structure of these metals have been done by cellular [1], augmented plane wave (APW) [2–5], linear muffin-tin orbital (LMTO) [6–8], non-relativistic APW [9], linearized augmented-plane-wave (LAPW) [10] and full-potential-augmented-plane-wave (FPAW) [11] methods. In addition to these, calculations are available where first principles density functional theory is used. However, the pseudopotential method [12] is relatively simple and is reasonably good for studying electronic properties of solids [13–18], especially of simple metals. For alkali and noble metals, pseudopotential does not deviate much from that of a free electron-like system [19]. On the other hand, for the transition metal, the choice of a model potential is generally found more reliable. In the pseudopotential procedure [20], the pseudowavefunctions are solved in the standard energy band calculations using pseudopotential. It is well known [12] that in the free electron-like solids, the pseudowave function resembles very closely the true wave function in the interatomic region. The model potential parameters are determined by fitting with experimental data. It is also known that a non-local

DOI: 10.1007/s12043-012-0301-x; ***e*Publication: 11 July 2012**

model potential describes the system better than a local model potential. In the calculation of Oli [21] using transition metal model potential of Heine–Abarenkov type, the density of states (G) and the electronic heat capacity (γ) for titanium and zirconium are not reported. The purpose of the present calculation is therefore to determine G and γ for these two metals. Ti and Zr which crystallize in hcp structure have the axial ratio of 1.59 (for ideal hcp, the ratio is 1.633). Energy band calculations are carried out using a model potential [22]. In order to test how good the present work is, a number of band structure-dependent properties, such as, the shape of the bands, the Fermi energy, G and γ are determined and compared with those available from experiment and other calculations.

The paper is divided into four sections. In §2, the theory is briefly outlined. Results and discussion are presented in §3. Conclusion is given in §4.

2. Theory

Ti and Zr have hcp structure at room temperature and at ambient pressure. At high pressure, and at room temperature, the hcp phase transforms to a more complex open hexagonal phase [9]. At high temperature, they exhibit body centred cubic (bcc) structure [8]. The most acceptable structure for Ti and Zr corresponding to the respective atomic configuration ($3d^2$, $4s^2$), ($4d^2$, $5s^2$) are usually chosen. The lattice constants [5,6] are tabulated in table 1. The unit cell which contains two atoms is displayed in figure 1. The c/a ratio is weakly volume-dependent in Ti but strongly dependent [10] in Zr. The Brillouin zone (BZ) is a hexagonal prism and has 24 equivalent parts connected to each other by the elements of the point-group D_{6h}. The irreducible part of the BZ is displayed in figure 2. The basic dimension (in au^{-1}) of BZ for Ti and Zr are taken from refs [2,19].

In the present work, the model potential method for energy band calculation [23] is used to determine the band energies and wave functions. In determining the energy and eigenfunctions of the conduction electrons, the Schroedinger equation,

$$H_{\mathrm{m}}|\chi_t(\vec{g})\rangle = E_t(\vec{g})|\chi_t(\vec{g})\rangle, \tag{1}$$

has been solved by quantum mechanical variational procedure. H_{m} is the model Hamiltonian, $|\chi_t(\vec{g})\rangle$ is the model wave function and E_t is the energy of the tth band at the $\vec{g}$ point in the BZ. In the atomic unit ($e^2 = 2, m = 1/2$ and $\hbar = 1$), the model Hamiltonian H is expressed as

$$H = -\nabla^2 + V_{\mathrm{m}}, \tag{2}$$

Table 1. Lattice constants of Ti and Zr.

Transition metal	Lattice parameter in atomic unit (au)			
(refs [5,6])	a	b	c	c/a
Ti	5.5754	5.5754	8.8502	1.59
Zr	6.106	6.106	9.728	1.59

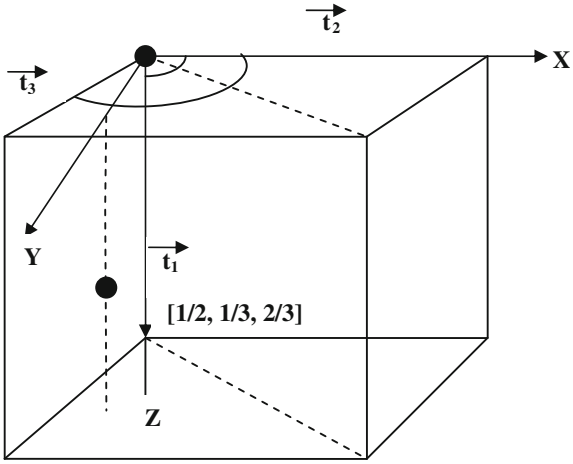

Figure 1. Unit cell of the hcp lattice in direct space indicating the position of two atoms.

where V_{m} is the model potential. This potential depends on the atomic volume through the energy parameters E [14]. The model potential reported by Animalu [22] is used in the present calculation. Model potential $V(q)$ is plotted in figure 3.

In variational procedure, the model wave function is expanded in a basis of plane wave,

$$|\chi_t(\vec{g})\rangle = \sum_{\vec{K}} C_t(\vec{g}, \vec{K}) \left|\mathrm{PW}(\vec{g} + \vec{K})\right\rangle, \tag{3}$$

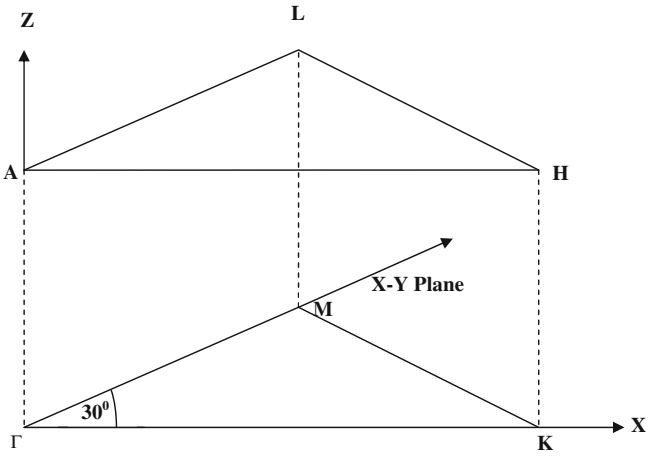

Figure 2. Irreducible part of the Brillouin zone of the hcp lattice.

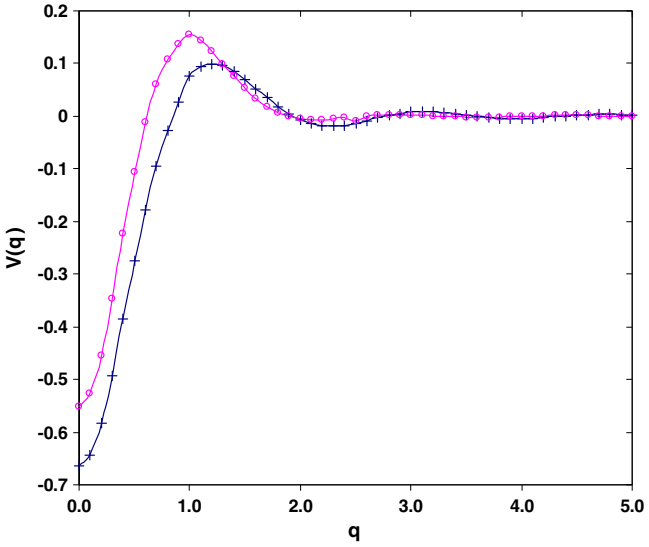

Figure 3. Variation of Fourier transform of model potential for Ti and Zr. The solid lines labelled by symbols + and ∘ represent Ti and Zr respectively.

where $\vec{g}$ is the wave vector in the reduced BZ, $\vec{K}$ is the reciprocal lattice vector, C_ts are the coefficients of linear combination and $|\mathrm{PW}(\vec{g}+\vec{K})\rangle$ is the plane wave basis vector. In the coordinate representation, the normalized plane wave is given by

$$\mathrm{PW}\,(\vec{g},\vec{r}) = \frac{1}{\sqrt{N\Omega}} \mathrm{e}^{i\vec{g}.\vec{r}}, \tag{4}$$

where N is the number of atoms in the solid and Ω is the volume per atom.

The energies $E_t(\vec{g})$ and the coefficients $C_t(\vec{g},\vec{K})$ are determined as a solution of the secular equation,

$$\left| H_{\vec{g}+\vec{K},\vec{g}+\vec{K}'} - E_t(\vec{g})\,\delta_{\vec{K}\vec{K}'} \right| = 0. \tag{5}$$

The size of the determinant is determined by the number of plane waves used in eq. (3) for the expression of $|\chi_t(\vec{g})\rangle$. This number is decided by the criterion of the convergence of energy and wave function. When the coefficients $C_t(\vec{g},\vec{K})$ are obtained, the model wave function $\chi_t(\vec{g})$ is completely determined. The true wave function $\psi_t(\vec{g})$ is determined by orthogonalizing the model wave function to all the core states. Once the band energies $E_t(\vec{g})$ are determined at the $\vec{g}$ points of BZ, the Fermi energy E_F is calculated by filling the band states from the lowest band energy upto which all the electrons in the solid are accommodated. The density of state ($G = \partial\aleph/\partial E$ where $\aleph$ is the number of states at energy E) is determined for both occupied and unoccupied band states. The electron heat capacity (γ) which is related to the density of states at E_F is calculated using the formula [24],

$$\gamma = \frac{1}{3}\pi^2 k_\mathrm{B}^2 N_0 G_\mathrm{cell}(E_\mathrm{F}), \tag{6}$$

where $N_0 (= N/2$ for Ti and Zr) is the number of cells, k_B is the Boltzmann's constant and $G_\mathrm{cell}(E_\mathrm{F}) = G(E_\mathrm{F})/N_0$ is the single cell contribution to the density of state at Fermi

energy. The latter is determined numerically using the energy of bands obtained in the present calculation.

3. Results and discussions

For selecting the representative $\vec{g}$ points, the wedge-shaped $\frac{1}{24}$th irreducible part of the BZ is divided into 6 parts by slicing it by equidistant planes perpendicular to C-axis. Each one of the six prisms is further divided into 64 sub-prisms of equal volume. In this way the irreducible part of BZ is divided into 384 sub-prisms. The centroid of each sub-prism is chosen as the $\vec{g}$-point. To each $\vec{g}$ point so chosen, a weighting factor in proportion to the volume it represents is assigned. The weighting factors are equal to $1/(24\times384)$. Thus the effective numbers of $\vec{g}$ points are 9216 in the complete BZ. Energy and eigenfunctions are calculated at each of these $\vec{g}$ points. The model wave function is expanded in 23 plane waves corresponding to the shortest 23 wave vectors $|\vec{g}+\vec{K}|$. Thus, the size of the matrix at each $\vec{g}$-point is 23×23. With this choice, the convergence of energy and eigenfunction is good. The energies of the occupied bands have converged to within 0.001 Ryd for both Ti and Zr. The band structures at the symmetry points are plotted for Ti and Zr in figures 4 and 5 respectively. The shapes of the band for Ti are compared with the other results [1,4,6]. Here the band structures are more or less similar to those from other band calculations [6]. Similarly, the shape of the band for Zr is compared with other results [1,5,7]. Here also the band structures are more or less similar to those from other energy band calculations [5]. The present results, however, differ substantially from those of Altmann and Bradley [1], Jepson [6,7], Loucks [5] as the energy bands are extremely sensitive to the choice of potential [5,25]. In the present method, the bands for Ti and Zr are very similar but there is an increase in bandwidth from Zr to Ti. The band structures obtained by LAPW method [10] using Hedin–Lundqvist form (HL), the exchange correlation potential, are identical with this method.

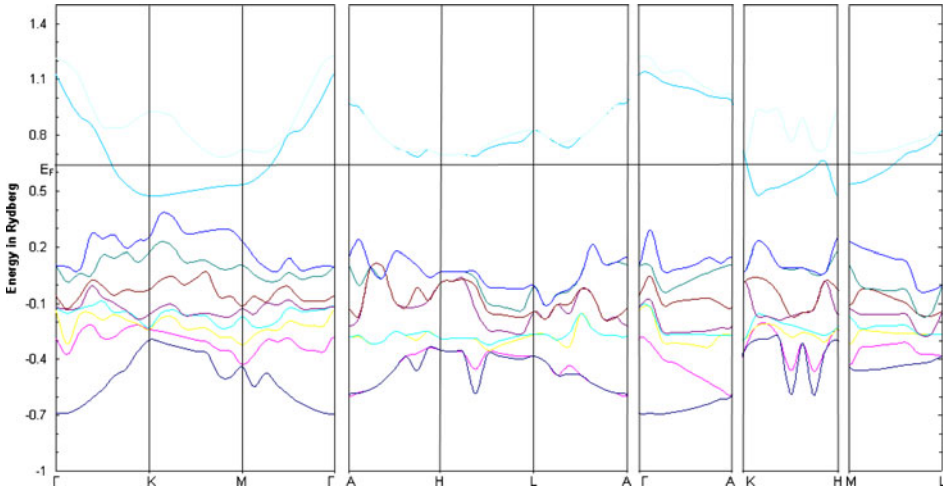

Figure 4. Energy bands for Ti along symmetry directions.

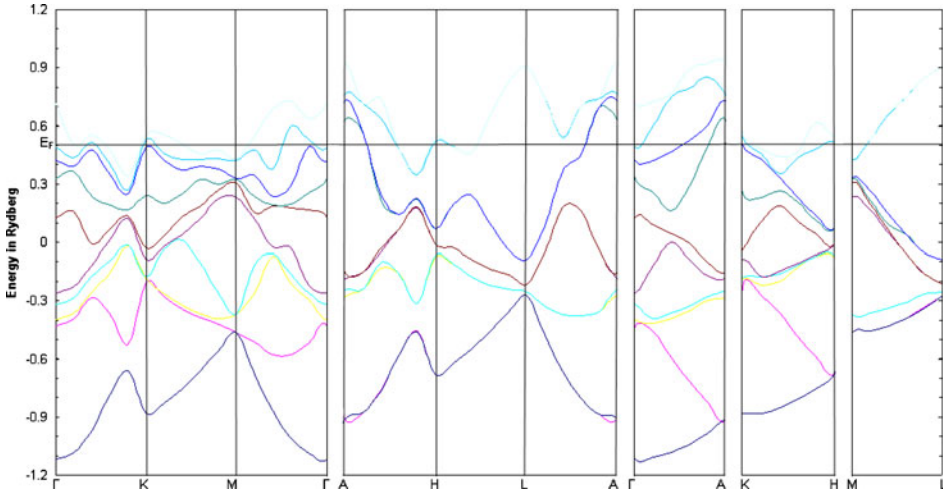

Figure 5. Energy bands for Zr along symmetry directions.

The density of state for Ti is plotted in figure 6 and for Zr in figure 7. The results E_F, $G(E_F)$, the density of states at E_F and $\gamma(E_F)$, the electronic heat capacity at E_F from the present calculation, other calculations and experiment, wherever available, are listed in tables 2 and 3 for Ti and Zr respectively. From these tables it is found that in the present method while E_F increases with bandwidth, both G and γ decrease. The variation of

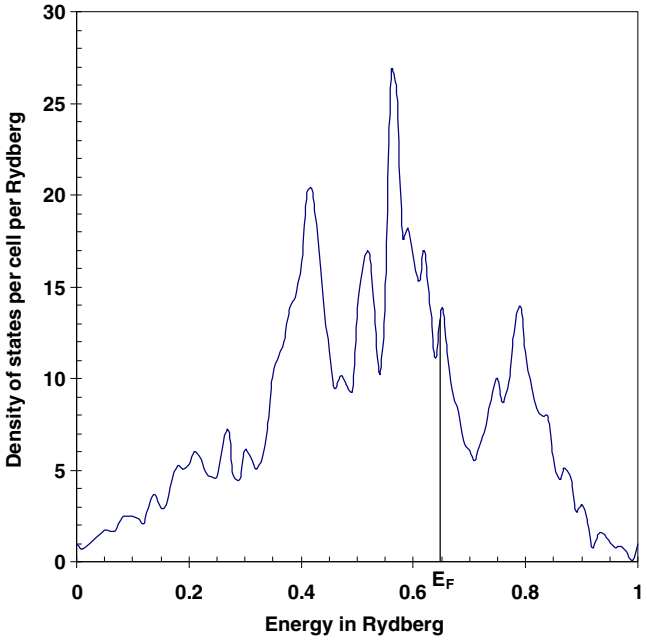

Figure 6. Density of states for Ti.

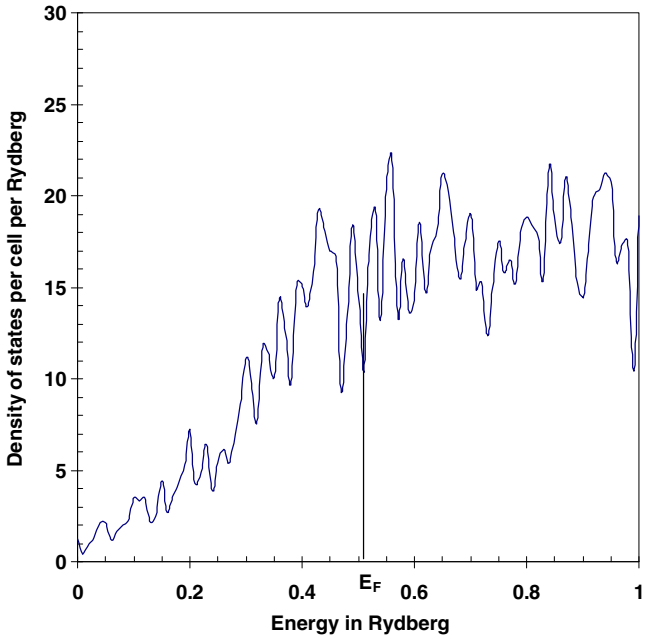

Figure 7. Density of states for Zr.

density of states with energy in the present calculation is very similar to those given by Jepson [6,7]. From tables 2 and 3, it is found that the ratio of $(\gamma/G)_{\text{exp.}}$ for Ti is 0.23 while for Zr it is 0.22. In the present method, on the other hand, $(\gamma/G)_{\text{Theory}}$ for Ti and Zr is 0.17 which is the same as measured in earlier methods [1,2,5–7,9] and obtained for free-electron case. In the present work, as the density of states at E_{F} in Zr is higher than that in Ti, the electronic heat capacity of Zr is larger than that of Ti. The ratio $\gamma_{(\text{Ti})}/\gamma_{(\text{Zr})}$ from the experiment is about 1.2. The ratio of the theoretical value to the present work is about 0.884 which is very close to the value from the relastivistic APW method. While the

Table 2. E_{F}, the Fermi energy, $G(E_{\text{F}})$, the density of states at E_{F}, γ, the electronic heat capacity, $\gamma_{\text{exp.}}$, the experimental heat capacity and γ_{Theory}, the theoretical electronic heat capacity in Ti from different calculations and experiment. E_{F} is expressed in Rydberg, $G(E_{\text{F}})$ in number of states/cell/Rydberg and γ in mJ/mole/K^2.

Parameters	Present result	Ref. [1]	Ref. [2]	Ref. [6]	Ref. [9]	Free-electron result	Expt. (refs [1,6])
E_{F}	0.65	0.30	0.33	0.67	0.31	0.99	Not available
$G(E_{\text{F}})$	12.88	38.60	28.50	12.40	14.80	12.04	14.40
$\gamma(E_{\text{F}})$	2.23	6.78	4.94	2.15	2.56	2.08	3.32
(γ/G)	0.17	0.17	0.17	0.17	0.17	0.17	0.231
$(\gamma_{\text{exp.}})/(\gamma_{\text{Theory}})$	1.49	0.49	0.67	1.54	1.29	1.59	

Table 3. E_F, the Fermi-energy, $G(E_F)$, the density of states at E_F, γ, the electronic heat capacity, $\gamma_{exp.}$, the experimental heat capacity and γ_{Theory}, the theoretical electronic heat capacity in Zr from different calculations and experiment. E_F is expressed in Rydberg, $G(E_F)$ in number of states/cell/Rydberg and γ in mJ/mole/K^2.

Parameters	Present result	Ref. [1]	Ref. [5]	Ref. [7]	Ref. [9]	Free-electron result	Expt. (refs [1,7])
E_F	0.51	0.40	0.39	0.60	0.31	0.83	Not available
$G(E_F)$	14.58	10.30	9.10	13.10	13.70	14.48	12.70
$\gamma(E_F)$	2.52	1.80	1.59	2.27	2.37	2.51	2.78
(γ/G)	0.17	0.17	0.17	0.17	0.17	0.17	0.22
$(\gamma_{exp.})/(\gamma_{Theory})$	1.10	1.54	1.75	1.22	1.17	1.11	

ratio of $\gamma_{expt.}$ to γ_{theory} for Ti is 1.48878, it is 1.10317 for Zr. This indicates an electron–phonon enhancement factor of about 1.5 for Ti and 1.1 for Zr, which is very reasonable as measured by Loucks [5]. It is found from the theoretical calculation that G and γ at E_F increase from Ti to Zr, while E_F decreases and this behaviour is not reflected by other methods except LMTO method.

4. Conclusions

Energy bands, Fermi energy, density of states and electronic heat capacity in the transition metals Ti and Zr are calculated using non-local model potential method. The results, particularly, the density of states at Fermi energy and the electronic heat capacity are found in reasonable agreement with the experiment. The difference between these results and experiment may be ascribed partly to contribution from phonons. Considering the relatively simple nature of the procedure and reasonably good accuracy of the results it produces, I conclude that this method may be applied with confidence to study other electronic properties such as electric field gradient in these metals.

Acknowledgements

It is pleasure to thank Professor N C Mohapatra for going through the manuscript and for many fruitful discussions and helpful comments.

References

[1] S L Altmann and C J Bradley, *Proc. Phys. Soc. London* **92**, 764 (1967)
[2] E H Hygh and Roland M Welch, *Phys. Rev.* **B1**, 2424 (1970)
[3] R M Welch and E H Hygh, *Phys. Rev.* **B4**, 4261 (1971)
[4] R M Welch and E H Hygh, *Phys. Rev.* **B9**, 1993 (1974)
[5] T L Loucks, *Phys. Rev.* **159**, 544 (1967)
[6] O Jepson, *Phys. Rev.* **B12**, 2988 (1975)
[7] O Jepson, O Krogh Anderson and A R Mackintosh, *Phys. Rev.* **B12**, 3084 (1975)

[8] I Bakoyni, H Ebert and A I Liechtenstein, *Phys. Rev.* **B48**, 7841 (1993)
[9] Y K Vohra, S K Sikka and R Chidambaram, *J. Phys. F: Metal Phys.* **9**, 1771 (1979)
[10] Zhi-Wei Lu, David Singh and Henry Krakaur, *Phys. Rev.* **B36**, 7335 (1987)
[11] P Blaha, K Schwarz and P H Dederichs, *Phys. Rev.* **B38**, 9368 (1988)
[12] W A Harrison, *Pseudopotential in theory of metals* (W.A. Benjamin Inc, Reading, Massachusetts, 1966)
[13] V Heine, *Solid State Phys.* **24**, 1 (1970)
[14] M H Cohen and V Heine, *Solid State Phys.* **24**, 37 (1970)
[15] B K Acharya and N C Mohapatra, *Pramana – J. Phys.* **43**, 391 (1994)
[16] B P Panda and N C Mohapatra, *Pramana – J. Phys.* **58**, 91 (2002)
[17] B P Panda and N C Mohapatra, *Pramana – J. Phys.* **61**, 1151 (2003)
[18] B P Panda and N C Mohapatra, *Physica* **B344**, 108 (2004)
[19] S L Altmann and C J Bradley, *Phys. Rev.* **A135**, 1253 (1964)
[20] B Mayer, K Hummler, C Elsässer and M Fähnle, *J. Phys. Condens. Matter* **7**, 9201 (1995)
[21] B A Oli, *J. Phys. F: Met. Phys.* **11**, 2007 (1981)
[22] A O E Animalu, *Phys. Rev.* **B8**, 3542 (1973)
[23] Joseph Callaway, *Quantum theory of solid state* (Academic Press, New York, 1974)
[24] C Kittel, *Introduction to solid state physics*, 5th edn. (Wiley, New York, 1976) p. 165
[25] K Iyakutti, C K Majumdar, R S Rao and V Devanathan, *J. Phys. F: Met. Phys.* **6**, 1639 (1976)